

Effect of mould speed on selected properties of moulded parts and energy consumption in rotational moulding

Karolina GŁOGOWSKA¹ , Filip LONGWIC¹, and Krzysztof LUDZIAK²

¹ Department of Technology and Polymer Processing, Faculty of Mechanical Engineering, Lublin University of Technology, Poland

² Department of Sustainable Transport and Powertrains, Faculty of Mechanical Engineering, Lublin University of Technology, Poland

Abstract. This paper deals with rotational moulding. The relationship between mould speed and wall thickness in the upper, middle and lower areas of rotational moulded parts is investigated. Young's modulus of moulded parts is determined via static tensile testing. A static compression test is performed to determine the maximum compressive force causing strain. The test is conducted on the wall of moulded parts, parallel to the main axis of rotation. Also, energy consumption in rotational moulding is investigated for different rotational speeds of the mould. Moulded parts are made of DOWLEX®2629UE linear low-density polyethylene (LLDPE). Experimental results are statistically analysed using STATISTICA 13. Non-parametric statistical tests are used for results analysis. The ANOVA method is employed to determine if there are any significant differences between obtained results. The statistical tests show that the range is much narrower for a speed ratio of 4:1. The narrowest range value is obtained for 12\3 rpm. The highest Young's modulus values are obtained for the parts moulded at 12\3 rpm (1263.33 MPa) and 16\4 rpm (1263.67 MPa). The highest maximum compressive force is obtained for the parts moulded at 12\3 rpm (10 400 N). An analysis of the results demonstrates that the part moulded at 12\3 rpm has the most advantageous properties. For this mould speed, the power consumption amounts to 8.28 kWh. Experimental results and statistical analyses demonstrate that mould speed affects both moulded part quality and energy consumption in the rotational moulding process.

Key words: rotational moulding; rotational speed; mechanical properties; compression.

1. INTRODUCTION

Processing of plastics can take place in commonly used devices such as extruders [1], injection moulding [2] machines and rotational moulding machines [3]. Rotational moulding, more commonly known as rotomoulding or rotocasting, is a low-pressure, high-temperature manufacturing process for producing hollow, one-piece plastic parts [4]. In rotational moulding, the mould performs a rotary or planetary motion about the main and auxiliary axes that are perpendicular to each other, or it rotates about its own axis while performing a swinging motion [5]. During rotational moulding, the speeds of rotation are slow, and the plastic effectively resides in the bottom of the mould until it is picked up by the mould wall to form a coating on the inside of the mould surface [6]. Rotational moulding is a cyclic process consisting of four stages: loading, heating, cooling and unloading [7].

Rotational moulding is used in industry to produce large volume parts without internal stresses [5]. Rotational moulding is one of few polymer processing techniques which does not require the use of complicated and expensive processing tools. Due to its many advantages, rotational moulding has a wide range of applications [8–10] and numerous studies are con-

ducted to optimize this method [11–13]. Rotational moulding is used to manufacture tanks and containers for fuel, chemicals and water, household waste-water treatment plants, food containers, instrument housings, medical equipment, road signs, toys, boats, canoes, and many more [14]. These types of products are nowadays primarily fabricated from polymeric materials. Polymers are used wherever other construction materials fail due to e.g. high costs, inadequate specific weight, poor chemical and corrosion resistance, or too complex processing.

Rotational moulded products can be used under difficult operating conditions [11, 15–17]. Therefore, studies must be conducted to investigate both properties of moulded parts and moulding process parameters affecting their physical and functional characteristics. The main technological parameters of rotational moulding include oven temperature, mould heating and cooling time, and mould speed. The essence of rotational moulding lies in finding an appropriate ratio between rotational speeds of the mould [18]. The speed ratio between different axes affects the pattern of polymer flow inside the mould cavity, powder mixing and distribution, as well as product wall thickness uniformity [19]. The technical knowledge about the effect of rotational moulding parameters such as rotational speed, speed ratio and mould geometry remain limited [19]. It must be stressed that the speed ratio, and rotation reversal if it is used, only affects material distribution during that stage of the heating cycle when the plastic is being laid up against the mould wall.

*e-mail: k.glogowska@pollub.pl

Manuscript submitted 2022-06-30, revised 2022-08-26, initially accepted for publication 2022-09-10, published in October 2022.

This occurs during the middle part of the oven stage, therefore speeds, speed ratios and rotation reversals are important currently. Once the plastic is in position against the mould wall, it is usually too viscous to move to any significant extent. The rotational speeds and the speed ratio are less critical toward the end of the process [20].

The typical speed range in rotational moulding is 4–20 rpm. The selection of appropriate rotational speeds for the mould is often done by trial and error [21]. To save time, a computer simulation package was developed especially for rotational moulding analysis [22]. The simulation package makes it possible to select the appropriate shape of a moulded part and predict the wall thickness of the part. The system is set up in the same way as the rotational moulding machine by entering data about rotation type (e.g. biaxial or rock and roll), mould position, mould speed, oven temperature, heating time, cooling type, cooling time, etc. The program then predicts the mould and internal air temperature profiles as well as the thickness of the part at every point on its surface [20].

Daryadel *et al.* concluded that rotational speed and processing temperature are the most important parameters during the rotational moulding process. And they are the most effective parameters on the studied tensile properties. They recommended using low rotational speed and high processing temperature as more helpful [23].

The study [24] used ANOVA and Taguchi to determine the optimal parameters of the rotational moulding process affecting strength properties. The study showed that the most important parameter is the rotational speed.

This paper presents the results of a study investigating the effect of the rotational speed of the mould on selected properties of moulded parts and energy consumption in rotational moulding. First, rotational moulding process parameters are described. Next, the relationship between the wall thickness of moulded parts and rotational speed of the mould is analysed. In addition to that, static tensile and compression tests are performed in order to determine Young's modulus and the maximum compressive force of moulded parts. Descriptive statistics and statistical tests are employed to interpret experimental results. Statistical analyses are performed using Statistica 13.

The literature review shows that the process variables play an important role in producing effective and reliable products in rotational moulding; however, no previous studies have investigated the relationship between rotational moulding process parameters and compression behaviour [25–29].

2. MATERIALS AND TECHNOLOGY

2.1. Material

Experiments were conducted on DOWLEX®2629UE linear low-density polyethylene (LLDPE) in powder form, manufactured by the Dow Chemical Company (Schkopau, Germany). The material has a melt mass flow rate of 4 g/10 min (190°C; 2.16 kg), tensile yield strength 17.5 MPa, strain at break 650%, flexural modulus 645 MPa (23°C) and Shore D hardness 57°Sh.

2.2. Rotational moulding process

The conditioning process involved drying LLDPE in a laboratory dryer for 24 h at 70°C. A total of 450 g of the material was used to fabricate moulded parts.

The rotational moulding process was conducted with the use of a single-arm spindle-type machine (Toruń, Poland) with two axes of rotation. The machine was equipped with a steel mould of cuboid shape. The mould had a wall thickness of 3mm. The test stand was provided with a meter for measuring the power supplied to the processing machine.

After filling the mould cavity with the required quantity of LLDPE, the mould was closed, rotated about the two axes and then put inside the oven. Eleven rotational speeds of the mould were applied to produce the moulded parts. These mould speeds on the major and auxiliary axes and their speed ratios are listed in Table 1. The oven temperature was set to 250°C. The mould with LLDPE specimens was heated for 20 min and then cooled in the air for 40 min.

The literature review shows that the most frequently used speeds range between 4 rpm and 20 rpm [9, 30, 31].

Table 1
Rotational speeds of the mould

Number	Axis speed		Coefficient
	Auxiliary axis speed rpm	Major axis speed rpm	
1	8	8	1:1
2	4		2:1
3	12	12	1:1
4	6		2:1
5	3		4:1
6	16	16	1:1
7	8		2:1
8	4		4:1
9	20	20	1:1
10	10		2:1
11	5		4:1

2.3. Measurements

The assessment of properties of moulded parts involved the following:

Measurements of the wall thickness of moulded parts. The EPOCH 4 ultrasonic flaw detector with a Panametrics v202-RM ultrasonic head (Warsaw, Poland) was used in the study. Wall thickness measurements were made for all moulded parts obtained with different rotational speeds. A total of 32 measurements were made on each moulded part: 8 measurements were made in the lower area of the part, 8 in the central area of the part, and 8 measurements were made in the lower area of the part. A schematic illustrating the way in which wall thickness was measured is shown in Fig. 1. In this paper only results obtained for one wall are presented – the one parallel to the main

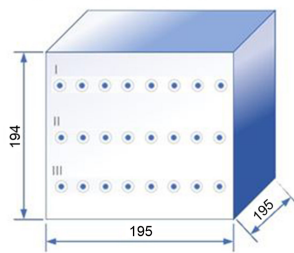


Fig. 1. Schematic drawing of a test piece and the location of wall thickness measurements

axis of rotation, because standard deviations obtained for individual walls had similar values.

Young's modulus was determined by a static tensile test conducted on a Zwick Roel Z101 testing machine (Ulm, Germany) in compliance with the ISO 527-1:2012 standard. Measurements were made on the wall parallel to the main axis of rotation (it was the same wall as that used for wall thickness measurements). Figure 2 shows sampling locations in the static tensile test.

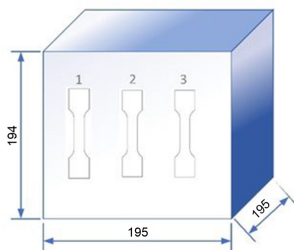


Fig. 2. Schematic drawing of a test piece and sampling location for static tensile test

A static compression test stand was designed especially for the purpose of this study. The Zwick Roel Z100 testing machine (Ulm, Germany) was equipped with two parallel plates to allow conducting the test on $195 \times 195 \times 194$ mm parts (Fig. 3). For each measurement the test piece was put on the plate in the same way, i.e. with the wall parallel to the main axis of rotation up front (it was the same wall as that used for wall thickness and Young's modulus measurements). The maximum compressive

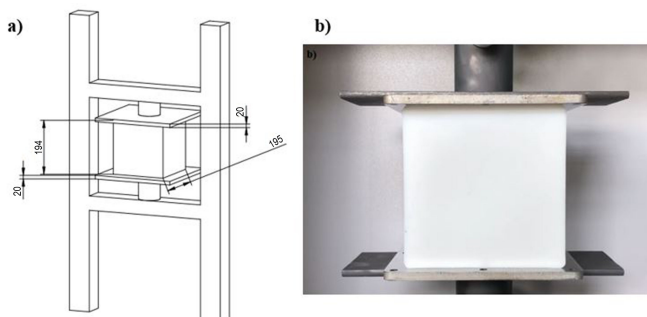


Fig. 3. Test stand for measuring maximum compressive force: a) schematic of the test stand, b) image of a test piece mounted in the grip

force (F_{\max}) was determined in the test. In the test, the traverse speed was 50 mm/min. The test was stopped when the maximum force dropped by 50% of its value.

Energy consumption in the rotational moulding process was calculated by measuring both the power supplied to the processing machine and moulding time. Measurements were made with the N43 meter from Lumel (Zielona Góra, Poland) and PowerVis software (Zielona Góra, Poland) dedicated for visualization, monitoring, archiving, and reporting power network parameters. The software is an integral part of the measurement system.

3. RESULTS AND DISCUSSION

This study investigated the effect of mould speed on the wall thickness and mechanical properties of moulded parts. However, for a comprehensive analysis of these properties, it was necessary to perform a statistical analysis of obtained data. The statistical analysis was performed using STATISTICA 13. The first step of the statistical analysis was descriptive statistics. Among others, the normality of the distribution of variables was tested. The Shapiro – Wilk W test was employed to verify the normality of distribution. When the tested variables did not meet the normal distribution condition, the non-parametric Kruskal–Wallis test was used for further analyses. To verify whether the above analyses confirmed the presence of statistically significant differences, a multiple comparisons test was performed. The significance level α assumed in the analyses was 0.05. For the significance coefficient α the verification procedure consisted of interpreting probability level p values obtained via respective tests.

3.1. Wall thickness results

First of all, wall thickness results obtained with different mould speeds were analysed statistically. Results of the Shapiro–Wilk W test are listed in Table 2. The Shapiro–Wilk W test results demonstrate that the probability level p in all groups is not greater than the assumed significance level of $\alpha = 0.05$. Therefore, it should be assumed that the obtained distribution greatly differs from the normal distribution.

The means were then compared using the Kruskal–Wallis and median tests. The Kruskal–Wallis and median tests are non-parametric equivalents of the parametric ANOVA. Statistical analysis results are given in Table 3.

For the assumed significance level α of 0.05, we decided to verify the null hypothesis stating that there were no significant differences between wall thickness values.

For the Kruskal–Wallis test the probability levels are as follows: $p = 0.0000$ for the upper area of a test piece, $p = 0.0054$ for the central area of a test piece, and $p = 0.0001$ for the lower area of a test piece. These probability levels are lower than the significance level $\alpha = 0.05$ for the upper and lower areas of a test piece, hence it can be concluded that the mean values for individual rotational speeds and wall thickness measurement locations are significantly different. As a result, there is a basis for rejecting the null hypothesis. The median test can be interpreted in a similar fashion.

Table 2
Results of the Shapiro–Wilk *W* test

Rotational speed, rpm	Place of measurement	<i>W</i> Shapiro–Wilk	<i>p</i> level for <i>W</i> Shapiro–Wilk
8\8	I	0.895119	0.260930
8\4		0.733427	0.005347
12\12		0.956312	0.774330
12\6		0.962369	0.832344
12\3		0.912414	0.371375
16\16		0.964106	0.848177
16\8		0.928379	0.501439
16\4		0.937938	0.590916
20\20		0.883785	0.204609
20\10		0.932065	0.535055
20\5		0.917412	0.409215
8\8		II	0.807564
8\4	0.956312		0.774330
12\12	0.886949		0.219156
12\6	0.911621		0.365618
12\3	0.907092		0.334041
16\16	0.789004		0.021805
16\8	0.899954		0.288683
16\4	0.892299		0.245803
20\20	0.945743		0.668312
20\10	0.820139		0.046821
20\5	0.918699		0.419395
8\8	III		0.836664
8\4		0.969952	0.969952
12\12		0.950989	0.721199
12\6		0.872036	0.157785
12\3		0.945433	0.665187
16\16		0.875864	0.171862
16\8		0.838963	0.073496
16\4		0.885483	0.212311
20\20		0.975058	0.934476
20\10		0.892567	0.247204
20\5		0.906679	0.331269

However, the test results do not indicate which groups are significantly different. In order to discover this, we employed a multiple comparisons method, which makes it possible to indicate significant differences in mean values for an assumed level of significance between independent groups. This method is employed if $p < \alpha$. The results of the multiple comparisons test are listed in Table 4.

The statistical test results show that significant differences between mean wall thicknesses in the upper area of the parts occur for the following speed ratios: 8\4 rpm – 16\4 rpm, 20\20 rpm – 20\5 rpm, and 20\20 rpm – 12\12 rpm. For the lower area of the part, significant differences are observed for the following speed ratios: 8\8 rpm – 8\4 rpm, and 12\3 rpm – 8\4 rpm – 20\10 rpm. No significant differences are observed for the central area of the moulded part. The results demonstrate that significant differences between the mean values exist between the lowest (8\4 rpm, 8\8 rpm) and highest (20\10 rpm and 20\20 rpm) mould speeds.

Wall thickness results are presented in box plots (Figs. 4–6). The plots show wall thickness as a function of measurement location (Fig. 1) and mould speed.

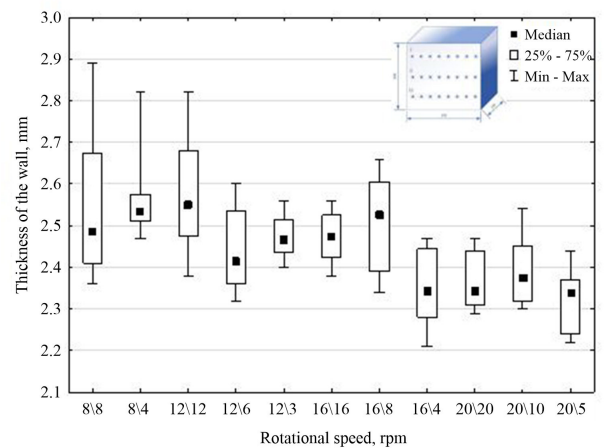


Fig. 4. Wall thickness versus rotational speed – upper area of a test piece

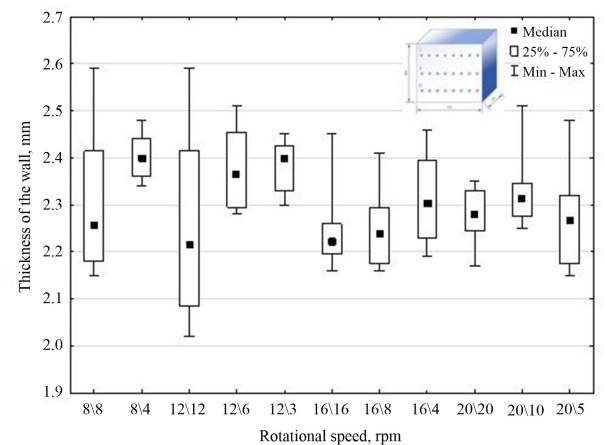


Fig. 5. Wall thickness versus rotational speed – central area of a test-piece

When investigating the relationship between mould speed and wall thickness, it is necessary to consider a measure of dispersion known as “range”. The range is the difference between the maximum and minimum wall thickness of a moulded part. The results demonstrate that the range is much narrower for

Effect of mould speed on selected properties of moulded parts and energy consumption in rotational moulding

Table 3
Results of the Kruskal–Wallis test

ANOVA rang Kruskala–Wallis test by rang: $H(10, N = 88) = 39.61, p = 0.0000$				$H(10, N = 88) = 24.96$ $p = 0.0054$			$H(10, N = 88) = 34.60$ $p = 0.0001$		
Rotational speed, rpm		Sum of ranks	Average rank		Sum of ranks	Average rank		Sum of ranks	Average rank
8\8	I	454.00	56.75	II	298.00	37.25	III	132.00	16.50
8\4		552.00	69.00		546.00	68.25		586.50	73.31
12\12		522.50	65.31		257.00	32.12		301.00	37.62
12\6		344.50	43.06		488.00	61.00		415.00	51.87
12\3		411.00	51.37		510.00	63.75		536.50	67.06
16\16		420.00	52.50		225.00	28.12		405.50	50.68
16\8		448.00	56.00		244.50	30.56		269.00	33.62
16\4		189.50	23.68		366.00	45.75		394.50	49.31
20\20		196.00	24.50		305.50	38.18		252.00	31.50
20\10		244.50	30.56		396.50	49.56		235.50	29.43
20\5		134.00	16.75		279.50	34.93		388.50	48.56

Table 4
Results of multiple comparisons for the Kruskal–Wallis test, obtained for lower and upper areas of a test piece

p values for multiple comparisons of test piece upper area Kruskal–Wallis test: $H(10, N = 88) = 39.61, p = 0.0001$											
	8\8	8\4	12\12	12\6	12\3	16\16	16\8	16\4	20\20	20\10	20\5
8\8		1.00	1.00	1.00	1.00	1.00	1.00	0.53	0.64	1.00	0.10
8\4	1.00		1.00	1.00	1.00	1.00	1.00	0.02	0.03	0.14	0.00
12\12	1.00	1.00		1.00	1.00	1.00	1.00	0.06	0.08	0.36	0.01
12\6	1.00	1.00	1.00		1.00	1.00	1.00	1.00	1.00	1.00	1.00
12\3	1.00	1.00	1.00	1.00		1.00	1.00	1.00	1.00	1.00	0.37
16\16	1.00	1.00	1.00	1.00	1.00		1.00	1.00	1.00	1.00	0.28
16\8	1.00	1.00	1.00	1.00	1.00	1.00		0.63	0.75	1.00	0.12
16\4	0.53	0.02	0.06	1.00	1.00	1.00	0.63		1.00	1.00	1.00
20\20	0.64	0.03	0.08	1.00	1.00	1.00	0.75	1.00		1.00	1.00
20\10	1.00	0.14	0.36	1.00	1.00	1.00	1.00	1.00	1.00		1.00
20\5	0.10	0.00	0.01	1.00	0.37	0.28	0.12	1.00	1.00	1.00	

p values for multiple comparisons of test piece upper area Kruskal–Wallis test: $H(10, N = 88) = 34.60, p = 0.0001$											
	8\8	8\4	12\12	12\6	12\3	16\16	16\8	16\4	20\20	20\10	20\5
8\8		0.00	1.00	0.31	0.00	0.41	1.00	0.56	1.00	1.00	0.66
8\4	0.00		0.29	1.00	1.00	1.00	0.10	1.00	0.06	0.03	1.00
12\12	1.00	0.29		1.00	1.00	1.00	1.00	1.00	1.00	1.00	1.00
12\6	0.31	1.00	1.00		1.00	1.00	1.00	1.00	1.00	1.00	1.00
12\3	0.00	1.00	1.00	1.00		1.00	0.49	1.00	0.30	0.18	1.00
16\16	0.41	1.00	1.00	1.00	1.00		1.00	1.00	1.00	1.00	1.00
16\8	1.00	0.10	1.00	1.00	0.49	1.00		1.00	1.00	1.00	1.00
16\4	0.56	1.00	1.00	1.00	1.00	1.00	1.00		1.00	1.00	1.00
20\20	1.00	0.04	1.00	1.00	0.30	1.00	1.00	1.00		1.00	1.00
20\10	1.00	0.03	1.00	1.00	0.18	1.00	1.00	1.00	1.00		1.00
20\5	0.66	1.00	1.00	1.00	1.00	1.00	1.00	1.00	1.00	1.00	

K. Głogowska, F. Longwic, and K. Ludziak

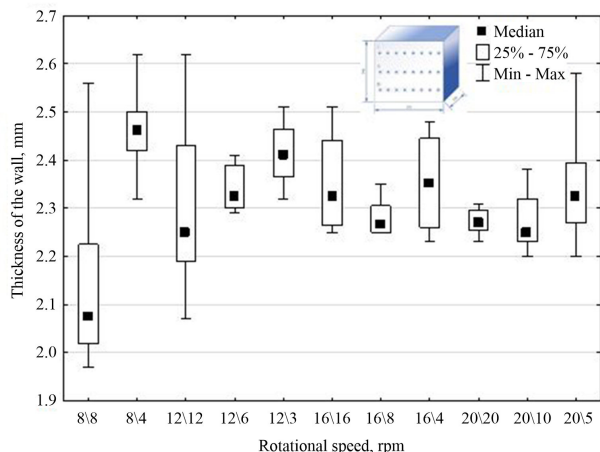


Fig. 6. Wall thickness versus rotational speed – lower area of a test-piece

a speed ratio of 4:1. The narrowest range value is obtained for 12\3 rpm. A complete statistical analysis of the effect of mould speed on wall thickness has not been previously reported in the literature. Different rotational speeds are reported in the literature. It can be said that these particular speeds were selected because the researchers considered them “appropriate”; however, there is no evidence that they are optimal.

The flow of the polymer inside the mould cavity depends on the applied rotational speeds and their ratio. If the rotational speed is too high, it may cause the polymer flow to become chaotic. This results in non-uniform wall thickness. The same effect may occur when the mould speed is too low. The flow of the polymer is static, and the material may be motionless at the bottom of the mould cavity.

3.2. Young's modulus of moulded parts

Values of Young's modulus of parts moulded at different rotational speeds were determined and compared. Figure 7 shows the obtained Young's modulus values.

Young's modulus is a basic measure describing the relationship between stress and strain in a material. Therefore, it was

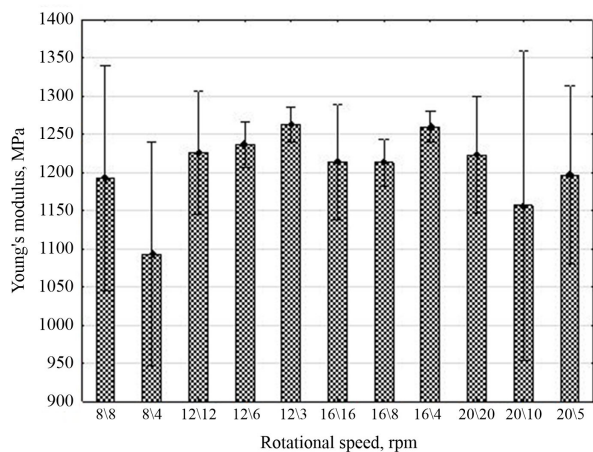


Fig. 7. Young's modulus of moulded parts

necessary to perform statistical analysis of the obtained results. Table 5 lists the results of descriptive statistics and Shapiro–Wilk test for the assumed significance level α of 0.05.

Table 5

Results of descriptive statistics and Shapiro–Wilk W test

Rotational speed, rpm	Young's modulus, MPa	Standard deviation	Variance	W Shapiro–Wilk statistics	Probability level p	Normal distribution
8\8	1216.67	95.04	9033.33	0.96	0.60	Yes
8\4	1103.33	86.22	7433.33	0.90	0.39	Yes
12\12	1226.67	40.41	1633.33	0.75	0.00	No
12\6	1236.67	15.28	233.33	0.96	0.64	Yes
12\3	1263.33	11.55	133.33	0.75	0.00	No
16\16	1213.33	37.86	1433.33	0.85	0.25	Yes
16\8	1203.33	30.55	933.33	0.96	0.64	Yes
16\4	1263.00	20.26	410.00	0.92	0.47	Yes
20\20	1223.33	20.82	433.33	0.96	0.64	Yes
20\10	1123.33	85.05	7233.33	1.00	0.94	Yes
20\5	1196.67	58.59	3433.33	0.88	0.33	Yes

An analysis of the results given in Fig. 7 and Table 5 reveals that the highest Young's modulus values are obtained for the parts moulded at 12\3 rpm (1263.33 MPa) and 16\4 rpm (1263.67 MPa). The lowest values of Young's modulus are obtained for the part moulded at 8\4 rpm (1103.33 MPa) and 20\10 rpm (1123.33 MPa). It can also be observed that the parts moulded at the lowest and highest mould speeds show the highest standard deviations. This is probably due to the non-uniform wall thickness of the parts produced at these speeds (Figs. 4–6).

The Shapiro–Wilk test results demonstrate that the normal distribution assumption is not met, therefore non-parametric tests are used in a further part of the analysis. To that end, the Kruskal–Wallis and median tests were employed, and their results are given in Tables 6 and 7.

For the Kruskal–Wallis test the probability level p is 0.0355, which is less than the assumed significance level of 0.05. Thus, it can be concluded that the average values obtained for individual parts are not the same. However, the results do not indicate which groups are significantly different. To that end, a multiple comparisons test was applied. Results of the multiple comparisons test are listed in Table 7.

The statistical test results demonstrate that significant differences in the mean Young's modulus values occur for the following mould speeds: 8\4 rpm – 12\3 rpm – 16\4 rpm, 12\3 rpm – 20\10 rpm as well as 16\4 rpm – 20\10 rpm. The probability level values are lower than the assumed significance level. For other mould speeds, the obtained Young's modulus values are not significantly different. The significance level is higher than the assumed one.

Effect of mould speed on selected properties of moulded parts and energy consumption in rotational moulding

Table 6

Results of the Kruskal–Wallis test by rank

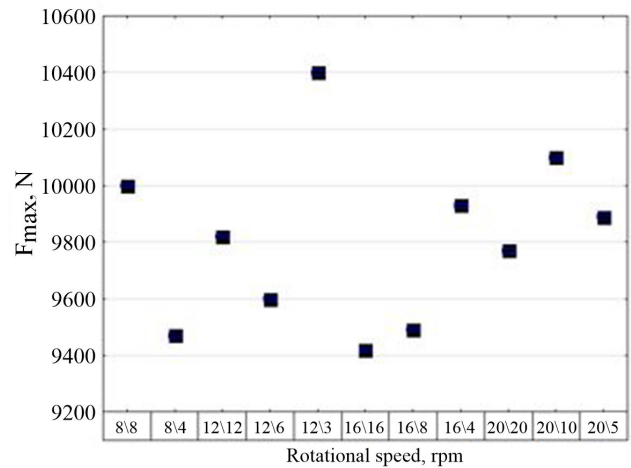
Kruskal–Wallis test, $p = 0.0355$		
Rotational speed, rpm	Sum of rangs	Average rank
8\8	52.00	17.33
8\4	14.00	4.83
12\12	61.50	20.50
12\6	61.50	20.50
12\3	86.00	28.67
16\16	45.50	15.17
16\8	37.00	12.33
16\4	85.00	28.33
20\20	58.00	19.50
20\10	18.00	6.00
20\5	41.50	13.83

The results show that the highest mean values and the lowest values of Young's modulus are obtained for a speed ratio of 4:1. The highest mean values of this property are observed for two speed ratios: 12\3 rpm (1263.33 MPa) and 16\4 rpm (1260.00 MPa). The lowest Young's modulus values are obtained for the parts which had a broad range of wall thicknesses. There exists a correlation between wall thickness uniformity and Young's modulus value.

The rotational speed and speed ratio determine the number of times a specific area on the mould wall passes through the powder bed and the direction in which it enters and exits the powder bed. This is crucial for the mechanical properties of the finished part such as tensile, impact, and flexural strength [32,33].

3.3. Compression test

The next stage of the study involved investigating the relationship between wall thickness uniformity/non-uniformity and compressive force (F_{max}). The maximum compressive force was determined by means of a static compression test. Obtained results are shown in Fig. 8.

**Fig. 8.** Maximum compressive forces

The highest maximum compressive force is obtained for the parts moulded at 12\3 rpm (10400 N), while the lowest value for the parts produced at 16\8 rpm (9420 N). An analysis of the wall thickness results reveals that the parts differ in maximum and minimum wall thicknesses. Non-uniform wall thickness can affect the maximum compressive force. All parts moulded with a speed ratio of 1:1 have similar compressive force values, i.e. 9820 N, 9817 N and 9770 N, respectively. The parts moulded with a speed ratio of 2:1 also have similar compressive force values.

Table 7

Results of multiple comparisons test

p values for multiple comparisons Kruskal–Wallis test. $p = 0.0355$											
Rotational speed, rpm	8\8	8\4	12\12	12\6	12\3	16\16	16\8	16\4	20\20	20\10	20\5
8\8		1.00	1.00	1.00	1.00	1.00	1.00	1.00	1.00	1.00	1.00
8\4	1.00		1.00	1.00	0.14	1.00	1.00	0.16	1.00	1.00	1.00
12\12	1.00	1.00		1.00	1.00	1.00	1.00	1.00	1.00	1.00	1.00
12\6	1.00	1.00	1.00		1.00	1.00	1.00	1.00	1.00	1.00	1.00
12\3	1.00	0.14	1.00	1.00		1.00	1.00	1.00	1.00	0.23	1.00
16\16	1.00	1.00	1.00	1.00	1.00		1.00	1.00	1.00	1.00	1.00
16\8	1.00	1.00	1.00	1.00	1.00	1.00		1.00	1.00	1.00	1.00
16\4	1.00	0.06	1.00	1.00	1.00	1.00	1.00		1.00	0.62	1.00
20\20	1.00	1.00	1.00	1.00	1.00	1.00	1.00	1.00		1.00	1.00
20\10	1.00	1.00	1.00	1.00	0.23	1.00	1.00	0.26	1.00		1.00
20\5	1.00	0.99	1.00	1.00	1.00	1.00	1.00	1.00	1.00	1.00	

Different strain modes were observed in the compression test. All test pieces are shown in Figs. 9–12.

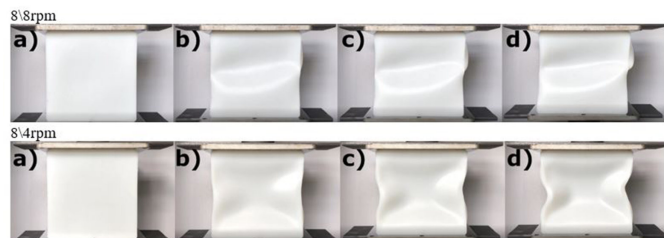


Fig. 9. Compression test conducted on parts moulded with speed ratios of 8\8 and 8\4 rpm, where: a) test piece at the start of the test, b) test piece after 10 s of testing, c) test piece after 15 s of testing, d) part after the compression test

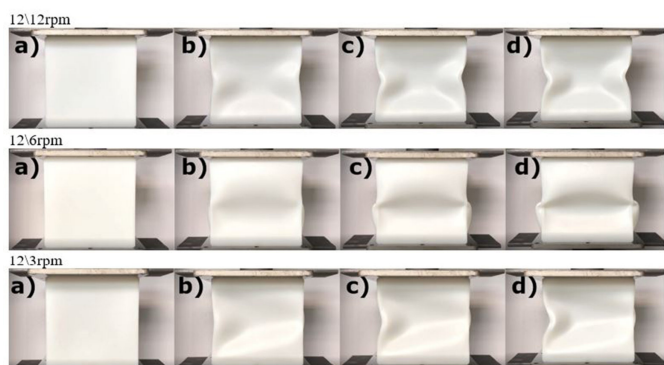


Fig. 10. Compression test conducted on parts moulded with speed ratios of 12\12, 12\6, and 12\3 rpm a) test piece at the start of the test, b) test piece after 10 s of testing, c) test piece after 15 s of testing, d) test piece after the compression test

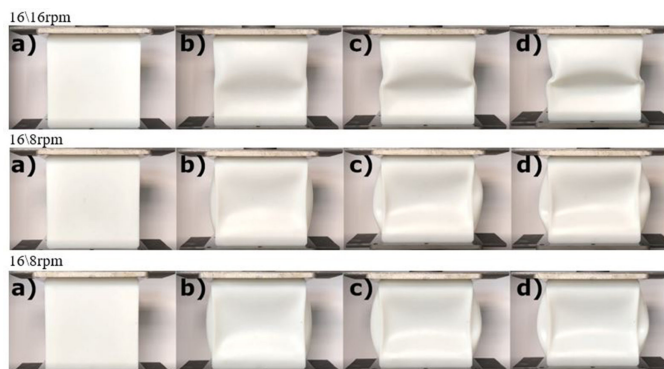


Fig. 11. Compression test conducted on parts moulded with speed ratios of 16\16, 16\8, and 16\4 rpm a) test piece at the start of the test, b) test piece after 10 s of testing, c) test piece after 15 s of testing, d) test piece after the compression test

The observed strain modes were classified as follows:

- L-shaped strain (8\8 rpm);
- X-shaped strain (8\4 rpm, 12\12 rpm);
- C-shaped strain (12\6 rpm, 16\16 rpm, 20\10 rpm);
- V-shaped strain (12\3 rpm);
- U-shaped strain (16\8 rpm, 16\4 rpm, 20\20 rpm, and 20\5 rpm).

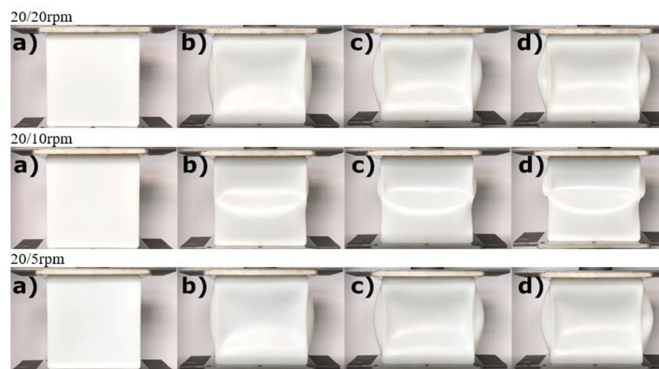


Fig. 12. Compression test conducted on parts moulded with speed ratios of 20\20, 20\10, and 20\4 rpm: a) test piece at the start of the test, b) test piece after 10s of testing, c) test piece after 15 s of testing, d) test piece after the compression test

One may speculate that there is a relationship between strain mode and compressive force. It can be observed that the parts exhibiting U-shaped strain have similar compressive force values, i.e. 9420 N, 9490 N, 9770 N, and 9450N, respectively. An analysis of the maximum compressive forces reveals a correlation between the wall thickness and Young's modulus value. The part with a narrow range of the wall thickness has the highest Young's modulus compressive force values. This part was moulded at 12/3 rpm.

Thus, the compression behaviour of LLDPE is significantly affected by its mechanical properties, which, in turn, depend on process parameters.

3.4. Energy consumption

Energy consumption in the rotational moulding process conducted with different rotational speeds of the mould is illustrated in Fig. 13. Although there are no significant differences between the results, certain relationships can be observed. It should be remembered that the energy consumption measurements were made on a laboratory machine. The differences in energy consumption values were considerably higher in the moulding process conducted under industrial conditions.

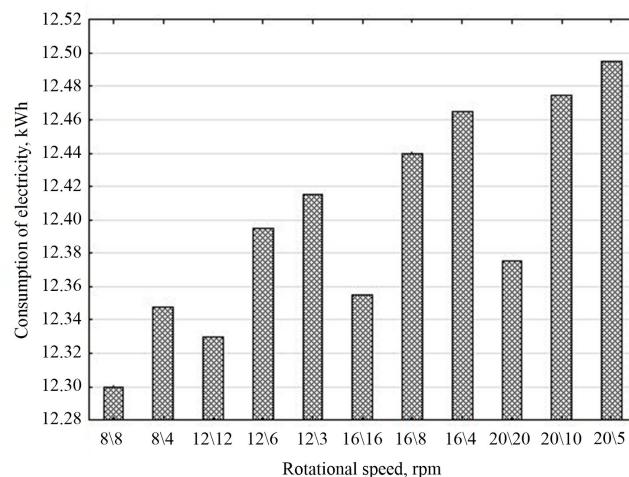


Fig. 13. Energy consumption versus rotational speed

Energy consumption increase depends on the mould speed on the main and auxiliary axes of rotation and their ratios (1:1, 2:1, 4:1). The highest energy consumption can be observed for the 4:1 speed ratio, while the lowest one for the speed ratio is 1:1. The highest increase in energy consumption is observed when the speed ratio is changed from 1:1 to 2:1. The higher the rotational speed on the main axis of rotation is applied, the higher the energy consumption becomes.

An analysis of the results demonstrates that the part moulded at 12\3 rpm has the most desirable properties. For this mould speed, the power consumption is 8.28 kWh.

Nowadays, for economic and ecological reasons, the engineering industry strives to reduce the energy consumption of production processes. It should be noted that a significant share of production costs is that of electricity. Consequently, the industry is looking for savings in this respect by purchasing energy-efficient machines or using energy-efficient production cycles. A change in mould speed may provide electricity savings.

4. CONCLUSIONS

Proper selection of parameters is one of the most important stages in rotational moulding. The aim of this study was to determine the effect of mould speed on wall thickness and selected properties of moulded parts. The study was conducted using 11 mould speeds in three ratios: 1:1, 2:1, and 4:1. The obtained results were interpreted by statistical analysis.

1. It is worth mentioning that with the appropriately selected mould speed, the moulded part will have a uniform wall thickness. This will result in improved mechanical and strength properties of the part, as confirmed by the experimental results. For the analysed rotational speeds, the optimum results were obtained at 12/3 rpm.
2. The moulded part had high values of Young's modulus and compressive force, which resulted from uniform wall thickness.
3. The statistical analysis results demonstrated that there were significant statistical differences between the obtained wall thicknesses and Young's modulus values.
4. Different strain modes were observed in the static compression test. Their shape could result from uniform/non-uniform wall thickness and Young's modulus value.
5. The study showed that the correctly selected mould speed could lead to reduced energy consumption.

The study described in this paper is limited to the biaxial rotation of a cuboid mould. Future studies should investigate whether similar results would be obtained if the mould had a different shape.

REFERENCES

- [1] D. Czarnicka-Komorowska, K. Bryll, E. Kostecka, M. Tomasiak, E. Piesowicz, and K. Gawdzinska, "The composting of PLA/HNT biodegradable composites as an eco-approach to the sustainability," *Bull. Pol. Acad. Sci. Tech. Sci.*, no. 69, p. e136720, 2021, doi: [10.24425/bpasts.2021.136720](https://doi.org/10.24425/bpasts.2021.136720).
- [2] S.K. Selvaraj, A. Raj, R. Rishikesh Mahadevan, U. Chadha, and V. Paramasivam, "A review on machine learning models in injection molding machines," *Adv. Mater. Sci. Eng.*, vol. 2022, p. 1949061, 2022, doi: [10.1155/2022/1949061](https://doi.org/10.1155/2022/1949061).
- [3] N. Gupta, P.L. Ramkumar, and V. Sangani, "An approach toward augmenting materials, additives, processability and parameterization in rotational molding: a review," *Mater. Manuf. Process.*, vol. 35, no. 14, pp. 1539–1556, 2020, doi: [10.1080/10426914.2020.1779934](https://doi.org/10.1080/10426914.2020.1779934).
- [4] R.J. Crawford and M.P. Kearns, *Practical Guide to Rotational Moulding*, Elsevier, 2021, p. 13.
- [5] P. Nugent, *18 – Rotational Molding*. William Andrew Publishing: 2011, pp. 311–332, doi: [10.1016/B978-1-4377-3514-7.10018-2](https://doi.org/10.1016/B978-1-4377-3514-7.10018-2).
- [6] R.J. Crawford and J.L. Throne, *Rotational Molding Technology*. William Andrew Publishing, 2001, p. 11.
- [7] P. Nugent, *Rotational molding: a practical guide*. William Andrew Publishing: 2001, pp. 809–811.
- [8] R.C. Vázquez Fletes *et al.*, "Morphological and mechanical properties of bilayers wood-plastic composites and foams obtained by rotational molding," *Polymers.*, vol. 12, no. 3, p. 503, 2020, doi: [10.3390/polym12030503](https://doi.org/10.3390/polym12030503).
- [9] P.S. Sari, S. Thomas, P. Spatenka, Z. Ghanam, and Z. Jenikova, "Effect of plasma modification of polyethylene on natural fibre composites prepared via rotational moulding," *Compos. B: Eng.*, vol. 177, p. 107344, 2019, doi: [10.1016/j.compositesb.2019.107344](https://doi.org/10.1016/j.compositesb.2019.107344).
- [10] J. Andrzejewski, A. Krawczak, K. Wesoly, and M. Szostak, "Rotational molding of biocomposites with addition of buckwheat husk filler. Structure-property correlation assessment for materials based on polyethylene (PE) and poly (lactic acid) PLA," *Compos. B: Eng.*, vol. 202, p. 108410, 2020, doi: [10.1016/j.compositesb.2020.108410](https://doi.org/10.1016/j.compositesb.2020.108410).
- [11] Y. Li, J.C. Liang, W. Zhang, W. Qi, M. Su, and C.D. Liu, "Study on process and impact strength for a rotationally molded truck fender," *J. Mater. Proces. Technol.*, no. 187–188, pp. 492–496, 2007, doi: [10.1016/j.jmatprotec.2006.11.142](https://doi.org/10.1016/j.jmatprotec.2006.11.142).
- [12] N. Gupta and P. L. Ramkumar, "Analysis of synthetic fiber-reinforced LLDPE based on melt flow index for rotational molding," *Advances in Lightweight Materials and Structures. Springer Proceedings in Materials*, 2020, vol. 8, pp. 599606, doi: [10.1007/978-981-15-7827-4_61](https://doi.org/10.1007/978-981-15-7827-4_61).
- [13] A. Mostafa, D.G.S. Sanchez, N. Sirach, R.V. Padilla, and H. Alsanat, "Analytical, numerical and experimental analysis of the creep behaviour of polyethylene polymers," in *International Conference on Numerical Modelling in Engineering*, Belgium, 2021.
- [14] G. Beall, *Rotational molding: Design, materials, tooling, and processing*. Hanser Verlag, 1998.
- [15] V. Sangeetha, D. Gopinath, R. Prithivirajan, V.G. Chandran, and R.M. Kumar, "Investigating the mechanical, thermal and melt flow index properties of HNTs–LLDPE nano composites for the applications of rotational moulding," *Polym. Test.*, vol. 89, p. 106595, 2020, doi: [10.1016/j.polymertesting.2020.106595](https://doi.org/10.1016/j.polymertesting.2020.106595).
- [16] G. Höfler, K. Jayaraman, and R. Lin, "Rotational moulding and mechanical characterisation of micron-sized and nano-sized reinforced high density polyethylene," *Key Eng. Mater.*, vol. 809, pp. 65–70, 2019, doi: [10.4028/www.scientific.net/KEM.809.65](https://doi.org/10.4028/www.scientific.net/KEM.809.65).
- [17] T. Ouprara and K. Sangpradit, "The development of rotational molding of waste bamboo powder with LLDPE plastic powder," in *E3S Web of Conferences, The 13th Thai Society of Agricultural Engineering International Conference*, Thailand, 2020.

- [18] G. Gogos, "Bubble removal in rotational molding," *Polym. Eng. Sci.*, vol. 44, no. 2, pp. 388–394, 2004, doi: [10.1002/pen.20035](https://doi.org/10.1002/pen.20035).
- [19] J. Adams, Y. Jin, D. Barnes, J. Butterfield, and M. Kearnes, "Motion control for uniaxial rotational molding," *J. Appl. Polym. Sci.*, no. 138, p. 49879, 2021, doi: [10.1002/app.49879](https://doi.org/10.1002/app.49879).
- [20] R.J. Crawford and M.P. Kearns, *Practical Guide to Rotational Moulding*. Elsevier: 2021, pp. 120–123.
- [21] J. Adams, Y. Jin, D. Barnes, and J. Butterfield, "Simulation the rotational moulding process using discrete element methods," in *IMC34 – 34th International Manufacturing Conference At: Sliigo Institute of Technology*, 2021.
- [22] J. Nieschlag *et al.*, "Experimental and numerical analysis of mold filling in rotational molding," *J. Compos. Sci.*, vol.5, no.11, p. 289, 2021, doi: [10.3390/jcs5110289](https://doi.org/10.3390/jcs5110289).
- [23] M. Daryadel, T. Azdast, M. Khatami, and M. Moradian, "Investigation of tensile properties of polymeric nanocomposite samples in the rotational molding process," *Polym. Bull.*, vol. 78, no. 5, pp. 24652481, 2021.
- [24] M.K. Raut and M.N. Raut, "A case study-optimization of plastic rotomolding process by anova and taguchi methods," *Ind. Eng. J.*, vol. 13, no. 12, pp. 39–44, 2020.
- [25] S.J. Liu and K.M. Peng, "Rotational molding of polycarbonate reinforced polyethylene composites: processing parameters and properties," *Polym. Eng. Sci.*, vol. 50, no. 7, pp. 1457–1465, 2010, doi: [10.1002/pen.21668](https://doi.org/10.1002/pen.21668).
- [26] A. Tcharkhtchi and J. Verdu, "Structure processibility relationships during rotational moulding of plastics," *Adv. Eng. Mater.*, vol. 6, no. 12, pp. 983–992, 2004, doi: [10.1002/adem.200400126](https://doi.org/10.1002/adem.200400126).
- [27] A. Marcilla, J.C. García-Quesada, R. Ruiz-Femenia, and M.I. Beltrán, "Crosslinking of rotational molding foams of polyethylene," *Polym. Eng. Sci.*, vol. 47, no. 11, pp. 1804–1812, 2007, doi: [10.1002/pen.20880](https://doi.org/10.1002/pen.20880).
- [28] M.J. Oliveira and G. Botelho, "Degradation of polyamide 11 in rotational moulding," *Polym. Degrad. Stab.*, vol. 93, no. 1, pp. 139–146, 2008, doi: [10.1016/j.polymdegradstab.2007.10.004](https://doi.org/10.1016/j.polymdegradstab.2007.10.004).
- [29] M. Kontopoulou and J. Vlachopoulos, "Melting and densification of thermoplastic powders," *Polym. Eng. Sci.*, vol. 41, no. 2, pp. 155–169, 2001, doi: [10.1002/pen.10718](https://doi.org/10.1002/pen.10718).
- [30] S.S. Abhilash, R. Luckose, and D.L. Singaravelu, "Processing and characterization of HDPE and MDPE processed by rotational, moulding," *Mater. Today: Proc.*, vol. 27, pp. 2029–2032, 2020, doi: [10.1016/j.matpr.2019.09.052](https://doi.org/10.1016/j.matpr.2019.09.052).
- [31] M.C. Cramez, M.J. Oliveira, and R.J. Crawford, "Effect of nucleating agents and cooling rate on the microstructure and properties of a rotational moulding grade of polypropylene," *J. Mater. Sci.*, vol. 36, no. 9, pp. 2151–2161, 2001.
- [32] M. Gupta, P.L. Ramkumar, and V. Sangani, "An approach toward augmenting materials, additives, processability and parameterization in rotational molding: a review," *Mater. Manuf. Process.*, no. 35, pp. 1539–56, 2020, doi: [10.1080/10426914.2020.1779934](https://doi.org/10.1080/10426914.2020.1779934).
- [33] P.L. Ramkumar, D.M. Kulkarni, and V.V. Chaudhari, "Parametric and mechanical characterization of linear low density polyethylene (LLDPE) using rotational moulding technology," *Sadhana*, vol. 39, no. 3, pp. 625–35, 2014, doi: [10.1007/s12046-013-0223-4](https://doi.org/10.1007/s12046-013-0223-4).